Tuesday, October 14, 2003
Morning Session I
MARS' PRESENT-DAY ATMOSPHERIC CIRCULATION
8:15 a.m. Victoria Room

REVIEW OF THE DAY'S AGENDA

Montmessin F. * Haberle R. M. Forget F. Rannou P. Cabane M.
Describing the Components of the Water Transport in the Martian Atmosphere **[#8089]**

Tyler D. * Barnes J. R.
Simulation of Atmospheric Circulations Over the Summertime North Pole Using the OSU Mars MM5 **[#8129]**

Keating G. M. * Theriot M. E. Jr. Tolson R. H. Bougher S. W. Forget F. Angelats i Coll M. Forbes J. M.
Recent Detection of Winter Polar Warming in the Mars Upper Atmosphere **[#8033]**

Colaprete A. * Haberle R. M.
Carbon Dioxide Convection in the Martian Polar Night and Its Implications for Polar Processes **[#8064]**

Bridger A. F. C. * Haberle R. M. Hollingsworth J. L.
Interannual Atmospheric Variability Simulated by a Mars GCM: Impacts on the Polar Regions **[#8111]**

PANEL DISCUSSION
PRESENT-DAY INTERANNUAL VARIATIONS
IN THE TRANSPORT OF CO_2, H_2O, AND DUST INTO THE MARTIAN POLAR REGIONS
Panelists: TBD

GENERAL DISCUSSION

10:15 – 10:30 a.m. BREAK

DESCRIBING THE COMPONENTS OF THE WATER TRANSPORT IN THE MARTIAN ATMOSPHERE.. F. Montmessin, R. M. Haberle, *NASA Ames Research Center - Moffett Field*, F. Forget, *Laboratoire de Meteorologie Dynamique-France*, P. Rannou, M. Cabane, *Service d'Aeronomie-France*.

Introduction: In this paper, we examine the meteorological components driving water transport in the Martian atmosphere. A particular emphasis is given to the role of residual mean circulation and water ice clouds in determining the geographical partitioning of water vapor and frost.

Model description: For our simulations, we use the General Circulation Model (GCM) developped at Laboratoire de Meteorologie Dynamique (Paris/France) [1] to simulate Martian hydrological cycle for various orbital configurations. The model includes usual representations of processes like surface sublmation, cloud formation and sedimentation (with predicted cloud particle sizes) [2]. Most of our simulations

Water cycle and circulation: Using the same decomposition as that found in [3], it is possible to recast the water transport in terms of circulation components. Indeed, it is staightforward to demonstrate that the total meridional transport of a tracer species includes the contribution of the mean meridional circulation, that of transient eddies and that of stationary waves.

Following this approach, we express the total transport of water vapor at a given latitude and at a given height as $[\bar{qv}]$, where the $\bar{qv}$ symbol denotes the time average and [] symbols denotes the zonal mean of the product qv, q being the mass mixing ratio of water and v the meridional wind. According to [3], $[\bar{qv}]$ can be written as:

$$[\bar{qv}] = [\bar{q}][\bar{v}] + [\bar{q'v'}] + [\bar{q^*v^*}] \quad (1)$$

with the prime symbol $'$ expressing the departure from the time average ($q' = q - \bar{q}$ and $v' = v - \bar{v}$) whereas the star symbol being related to the departure from the zonal average ($q^* = q - [q]$ and $v^* = v - [v]$).

In short, total water transport $[\bar{qv}]$ is the sum of the mean meridional circulation component $[\bar{q}][\bar{v}]$, that of transient eddies $[\bar{q'v'}]$ and that of non-travelling waves $[\bar{q^*v^*}]$. Eq. (1) can be integrated over height to yield

$$\int_{p_s}^{0} [\bar{qv}]\frac{dp}{g} = \int_{p_s}^{0} [\bar{q}][\bar{v}]\frac{dp}{g} + \int_{p_s}^{0} [\bar{q'v'}]\frac{dp}{g} + \int_{p_s}^{0} [\bar{q^*v^*}]\frac{dp}{g} \quad (2)$$

The latter equation, akin to a zonal- and vertical-mean expression of the water meridional transport, synthetizes the general behavior of the meridional flux fields. Given that q is the sum of both atmospheric water vapor and water ice (clouds), eqs. (1) and (2) can be further recasted to yield the respective contributions of vapor and clouds. Most of the water cycle studies to date [4,5] have focused on the sole role of the Hadley cell in cross-equtorial flows of moisture. However, [4] and [5] have shown that baroclinic activity plays a key role in cycling water in and out the north residual cap. Indeed, [6] concluded that the observed extraction of water from the north polar cap can not be reproduced with a two-dimensionnal circulation model. According to [5], horizontal mixing of moisture between high and mid-latitudes precedes the incorporation of water within the ascending branch of the Hadley cell in the northern tropics. Likewise, the mechanism by which water returns to the north residual cap includes water trapping in the seasonal CO_2 cap, thanks to an intense mixing of air masses across the cap edge. During the recession of the cap, seasonal water frost is carried poleward by a succession of sublimation/recondensation processes occuring within poleward warm fronts and equatorial cold fronts.

With this in mind, describing water transport in terms of its meteorological components becomes a necessary task in order to fully appreciate the mechanisms controlling the Martian water cycle stability.

Results of our analysis on an annual average and at specific seasons will thus be presented.

Water cycle and clouds: Following their first observation of what has been since called the "Aphelion cloud belt", i.e. a cloudy structure encircling the equator during northern spring and summer, [7] proposed a mechanism, involving clouds, to predict preferred storage location of water with changes of perihelion date. The so-called *Clancy effect* comes from the potential ability of clouds to sequester water below the returning branch of the equinoctial Hadley cell if the latter is synchronized with the aphelion season. In practice, aphelion season implies decreasing atmospheric temperatures in the tropics and thus lower levels of condensation/precipitation. Perihelion season, on the contrary, comes with enhanced solar forcing and warmer temperatures which allow water to be carried by the Hadley cell towards the winter hemisphere without experiencing the effects of cloud sedimentation.

On an annual average, [7] suggests a net flux of water towards the hemisphere for which summer is timing with aphelion. Whereas the current orbital configuration should therefore favor the northern hemisphere, it also implies that this situation is reversed when the perihelion is shifted of 180^o.

[7] even suggested that the current position of the permanent water ice cap is a consequence of this effect. Accordingly, the permanent water ice cap should move to the south pole when aphelion occurs during southern summer.

On the other hand, [8] showed that, regardless of excentricity and aphelion date, the south to north topographic slope applies a major component to the general circulation biasing cross-equatorial mass flows towards the north hemisphere.

The purpose of our study is to confront the *Clancy effect* to that induced by topographic forcing within the context of GCM simulations. Ultimately, we will discuss the stability of a permanent cap in the south pole that recent observations may confirm [9].

Reference

[1] F. Forget et al., *JGR* **104**, 24155 (1999)

[2] F. Montmessin et al., *proceedings of the mars VI conference*, Pasadena (2003)

[3] J. P. Peixoto and A. Oort, *Physics of Climate*, Amer. Inst. of Physics (1992)
[4] H. Houben et al., *JGR* **102**, 9069 (1997)
[5] M. Richardson and J. Wilson, *JGR* **107**, 10.129/2001JE001536 (2002)
[6] R. Haberle et B. Jakosky, *JGR* **95**, 1423 (1992)
[7] T. Clancy et al., *Icarus* **122**, 36 (1996)
[8] M. Richardson and J. Wilson, *Nature* **416**, 298 (2002)
[9] T. Titus et al., *Science* **299**, 1048 (2003)

SIMULATION OF ATMOSPHERIC CIRCULATIONS OVER THE SUMMERTIME NORTH POLE USING THE OSU MARS MM5. D. Tyler[1] and J. R. Barnes[2], [1]College of Oceanic and Atmospheric Sciences, Oregon State University, dtyler@coas.oregonstate.edu; [2]College of Oceanic and Atmospheric Sciences, Oregon State University barnes@coas.oregonstate.edu.

Introduction: It is important to develop a more thorough knowledge of mesoscale circulations over the residual polar ice caps of Mars. Mesoscale circulations, forced by topography and gradients in the thermal properties of the surface, can significantly modify surface energy fluxes throughout these regions on relatively small scales. Efforts to more completely describe polar weather and climatology, at resolutions greater than those of present day General Circulation Models, must account for the importance of mesoscale circulations. Moreover, a greater understanding of polar mesoscale circulations will assist other investigations into polar processes. This research is the first comprehensive high-resolution attempt to understand the dynamics of the north polar summertime circulation

Mars MM5 Simulations: We have used the OSU Mars MM5 (MMM5) [1] to simulate atmospheric circulations, for northern hemisphere summertime conditions, over the north residual ice cap and southward into midlatitudes. The model was run hydrostatically using a semi-global mother domain, and two-way nesting was used to resolve circulations over Chasma Boreale to a resolution of ~6 km. Three simulations (14 sols each) were performed for L_s values of: 90°, 135° and 160°. Only the final eight sols of each simulation (output centered on L_s values) were used for analysis. Together these simulations allow an examination of how atmospheric circulations change during the entire season that the north residual ice cap is exposed to the atmosphere.

Both the MMM5 and the NASA Ames Mars GCM [2], which is used for boundary and initial conditions, utilize the most current thermal inertia [3], albedo [4] and topography [5] data that is presently available. Our model was tuned to match Radio Science temperature profiles for Ls=135° [6]. The MMM5 was tuned by first setting the visible dust opacity in the model to coincide with TES IR opacities for dust [7], and then by fixing the deepest soil model temperature for ice surfaces (dependent upon albedo) to an appropriate mean climatological temperature (175 K). Subsurface heat flux can play an important role in the residual cap energy budget [8], and this change in the initialization routines of the MMM5 yields simulated residual cap temperatures that match quite favorably with the TES observations without modifying albedo values.

Results: At the time of this writing an analysis of model results is in progress. With three runs, each at multiple resolutions (nesting), we have a 6-D data set. However, there are some results from this analysis that deserve preliminary comment.

Zonal means. Zonal Mean fields from the MMM5 are quite similar with those from the NASA Ames Mars GCM in the lower to middle atmosphere, especially over polar regions when comparing with the coarse resolution results of the MMM5 mother domain (~162 km). At a resolution nine times that of the mother domain (~18 km, two nests in), the winds over the residual cap become well resolved, with zonal mean values at L_s=90° that exceed 10 ms^{-1} near the surface over much of the cap, see Fig. 1. Such wind speeds have been suggested as possibly being required to move the amount of water off the residual cap that was measured by MAWD [9]. By late summer, Ls=135°, mean wind speeds drop to ~5 ms^{-1}, significantly reducing the wind stress on the residual cap.

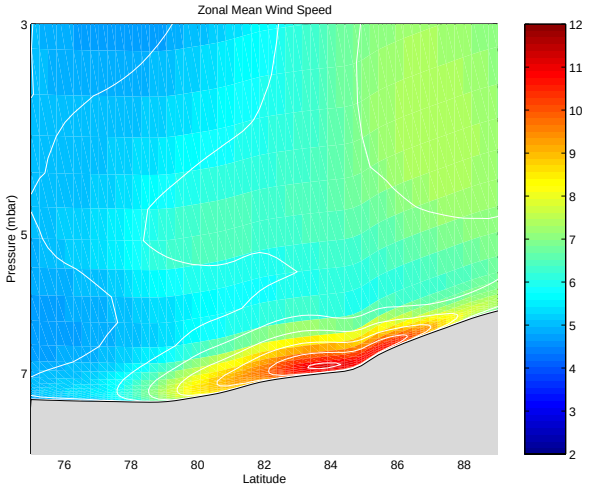

Figure 1: Eight-sol zonal mean wind speeds, for L_s=90°, over the north residual ice cap. The plot was constructed by averaging data on sigma surfaces and then converting the vertical coordinate of the average to pressure. The resolution of this nest is ~18 km.

The zonal mean meridional wind field over the residual cap is weak, as is the zonal mean zonal wind field. At the surface we do observe a weak and fairly shallow off-cap flow, with speeds of ~3 ms^{-1}. Zonal winds contribute most significantly to the zonal mean

wind speeds near the residual cap surface. Aloft, above the residual cap, the zonal mean meridional and zonal winds are negligible, suggesting there is little meridional mixing of the polar atmosphere into lower latitudes. This is only correct in terms of the zonal mean wind fields. For diurnal mean slices at specific longitudes, or for instantaneous meridional winds throughout the course of the day, the results differ dramatically from the zonal means.

Diurnal means and diurnal cycles. Diurnal mean meridional slices of meteorological fields (T, U and V) exhibit a substantial amount of asymmetry from their respective zonal means. As would be expected, we find that some of the strongest off-cap meridional flows are concurrent with Chasma Boreale.

Asymmetries from the zonal mean winds can become surprisingly large at latitudes just south of the residual cap. Certain longitudes exhibit fairly deep northerly or southerly diurnal mean flow (~5 ms^{-1}). At higher altitudes in the modeled atmosphere, asymmetries from the zonal mean meridional flow are also quite pervasive.

Presently we are investigating dynamical mechanisms to better understand the causes for these asymmetric features of the polar circulation in our model. Larger scale dynamics are presumably involved, possibly related to the proximity of Alba Patera and the Tharsis massif. This seems the single most impressive topographical feature that is close enough to be dynamically significant in the polar circulation. A working hypothesis is that stationary features of a larger scale circulation are influencing the smaller scales.

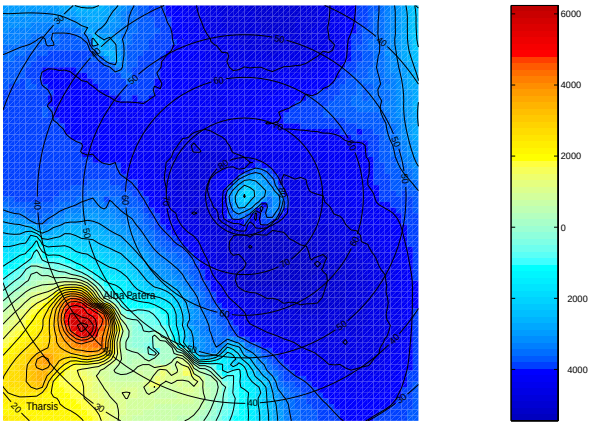

Figure 2: Topography of the ~54 km nest that was used in these simulations (76x76).

An interesting aspect of the polar circulation that we hope to understand is what we have described as "tidal sloshing" [10]. Meridional winds, in the bulk of the atmosphere above the residual cap, reverse direction over the course of the diurnal cycle with a dominant diurnal period. The strength of this effect has longitudinal preference, but it is a pervasive phenomenon over the entire north polar cap in these simulations. The image in Fig. 2 shows topography of the first nest below the mother domain (~54 km); the image is suggestive of why we are suspicious of large-scale dynamical influences related to the proximity of Alba Patera and Tharsis.

Future Direction: This work, when finalized, will complete my Ph.D. studies. Our next effort in this research will be to activate water transport in the MMM5, correctly configure the associated water routines in the model, and revisit these same simulations with the objective of developing a better understanding of the atmospheric pathways through which water is transported southwards off the north residual cap in northern hemisphere summer. There is much to be learned about the present day stability of the residual ice caps using such models, and we look forward to working closely with others interested in investigating the stability and evolution of polar ice deposits.

References: [1] Tyler D. and Barnes J. R. (2002) *JGR, 107,* 10.1029/2001JE001618. [2] Haberle R. M. et al. (1999), *JGR*, *104*, 8957-8974. [3] Mellon M. T. et al. (2002) *LPS XXXIII, Abstract #1416*. [4] Christensen P. R. et al. (2001) *JGR*, *106*, 23,823-23,871. [5] Smith D. E. et al. (1999) *Science*, *284*, 1495-1503. [6] Hinson D. P. et al. (2001) *JGR*, *106*, 1463-1480. [7] M. Smith, *Submitted to Icarus*, (2003). [8] Paige D. A. and Ingersoll A. P. (1985) *Science*, *228*, 1160-1168. [9] Haberle R. M. and Jakosky (1999), *JGR*, *102*, 9069-9083. [10] Tyler D. and Barnes J. R. (2003), *Granada Mars Workshop*.

RECENT DETECTION OF WINTER POLAR WARMING IN THE MARS UPPER ATMOSPHERE

G. M. Keating, M. E. Theriot, Jr., and R. H. Tolson, *George Washington Univ. Campus at NASA Langley, Hampton, VA 23681 USA (g.m.keating@larc.nasa.gov),* S. W. Bougher, *Univ. of Michigan, Ann Arbor, MI, USA,* F. Forget and M. Angelats i Coll, *Univ. of Paris, Lab. de Meteorologie Dynamique, Paris, France*, and J. M. Forbes, *Univ. of Colorado, Boulder, CO, USA.*

The Mars Global Surveyor (MGS) z-axis accelerometer has obtained over 1600 vertical structures of thermospheric density, temperature, and pressure, ranging from 110 to 170 km, between Sept. 1997 and March 1999, compared to only three previous such vertical structures from Viking 1, 2, and Pathfinder [1]. In November 1997, a regional dust storm in the Southern Hemisphere triggered an unexpectedly large thermospheric response at mid-northern latitudes, increasing the altitude of thermospheric pressure surfaces there by as much as 8 km and indicating a strong global thermospheric response to a regional dust storm [2].

From analysis of the MGS accelerometer data, enormous planetary scale waves have been detected in the Martian thermosphere between 60°N and 60°S. Fourier analysis of the wave structure reveals high amplitude waves 2 and 3 which appear to remain at nearly constant longitude between ± 60° latitude when viewed near 3 PM [3,4]. However, measurements near 3 AM show evidence of essentially a phase reversal in wave 2 [3]. Taking into account the near sun-synchronous orbit it appears that these waves are principally non-migrating tides propagating to the east. Studies by Wilson et al. [5] and Forbes et al. [6] indicate the wave 2 component observed from MGS is principally an eastward propagating diurnal wave 1 which rotates around Mars in the opposite sense of the sun once per day. The wave 1 Kelvin wave principally results from the interaction of tides and topography. Analysis of Thermal Emission Spectrometer (TES) MGS data near 30 km [5] indicates a similar phase to this wave at 30 km [5], which is in accord with the Kelvin wave, and thus the wave appears to propagate up from below into the thermosphere. The observed wave 3 may be a combination of an eastward propagating, semi-diurnal wave 1 and the eastward propagating, diurnal wave 2 (basically the wave 2 Kelvin wave). Both the observed wave 2 and wave 3 maximize near the equator. These results give further evidence of coupling between the lower and upper atmosphere.

The Mars Odyssey 2001 (M01) Spacecraft was placed into orbit about Mars in September 2001. Aerobraking was performed from then until January 2002 to circularize the M01 orbit. The spacecraft carried triaxial accelerometers, which were used to safely perform aerobraking and to continue exploration of the detailed properties of the upper atmosphere, which had begun with the Mars Global Surveyor accelerometer measurements. The accelerometers were used to measure atmospheric density, and from the vertical structures measured on both inbound and outbound trajectories the scale height, temperature and pressure were determined. Altogether 600 vertical structures were obtained ranging from 95 km to above 170 km. Measurements were obtained for the first time near the North Pole. Also, the first measurements were obtained on the night-side in the Northern Hemisphere. Temperatures near 110 km were discovered to increase with latitude maximizing near the North winter pole, apparently due to dynamical heating [7]. This result is contrary to the MarsGram and MTGCM models used for Odyssey aerobraking, where model temperatures are predicted to minimize near the winter pole. For example, maximum temperatures near the North winter pole at 100 km were observed to be near 200 K while MTGCM temperatures were predicted to be near 100 K. However, an upper atmosphere winter polar warming is predicted by the European Mars GCM [8] at both the North and South Poles in local winter at high altitudes. The altitudinal variations and high latitude diurnal variations of temperature near the North Pole also appear to be in fair accord with the Forget et al. model. Apparently, the upper atmosphere North polar winter warmings may result from adiabatic heating from the subsiding branch of the cross-equatorial meridional circulation from the Southern Hemisphere summer. The only measurements of the Southern Hemisphere winter polar upper atmospheric temperatures were obtained from accelerometers aboard the Mars Global Surveyor. These measurements do not show winter polar warmings, but minimum temperatures near the winter South Pole more in accord with radiative equilibrium, and more in

accord with the MTGCM model. Apparently, the summer-to-winter cell supplying dynamical heating to the North winter pole near perihelion is much stronger than the summer-to-winter cell supplying dynamical heating to the South winter pole near aphelion. The stronger dynamical heating during the North polar winter may result from being near perihelion where the closer sun and stronger dust activity may strengthen the meridional cell.

Previously, intense warming of the winter polar atmosphere was observed in the lower atmosphere (~25km) by the Infrared Thermal Mapper Instrument (IRTM) aboard the Viking orbiters during the onset of the 1977b global dust storm at northern hemisphere winter solstice [9,10].

References

[1] R. H. Tolson, G. M. Keating, et al. (1999) Application of accelerometer data to Mars Global Surveyor aerobraking operations, J. of Spacecraft and Rockets, 36, No. 3.

[2] G. M. Keating, et al. (1998) The structure of the upper atmosphere of Mars: In Situ accelerometer measurements from Mars Global Surveyor, Science, 279, 1672.

[3] G. M. Keating, et al. (2001) Persistent planetary-scale wave-2 and wave-3 density variations observed in Mars upper atmosphere from MGS accelerometer experiment, Proceedings of European Geophysical Society, 78, 229.

[4] S. W. Bougher, G. M. Keating, et al. (2001) The upper atmosphere wave structure of Mars as determined from Mars Global Surveyor Accelerometer, EOS, Trans, AGU, supplement, page F717.

[5] R. J. Wilson. (2002) Evidence for nonmigrating thermal tides in the Mars upper atmosphere from the Mars Global Surveyor accelerometer experiment, Geophys Res. Lett., 29, (7), 10.1029 GL013975.

[6] J. M. Forbes, G. M. Keating, et al. (2002) Nonmigrating tides in the thermosphere of Mars, In Press, J. Geophys. Res., Planets.

[7] G. M. Keating, et al. (2002) Detection of North Polar winter warming from the Mars Odyssey 2001 accelerometer experiment, Proceedings of the 34th Scientific Assembly of the Committee on Space Research (COSPAR) and the World Space Congress, 142.

[8] F. Forget, et al. (1999) Improved general circulation models of the Martian atmosphere from the surface to above 80 km, J. Geophys Res., 104, 24155.

[9] B. M. Jakosky and T.Z. Martin. (1987) Mars: North-polar atmospheric warming during dust storms, Icarus,72,528.

[10] R. J. Wilson. (1997) A general circulation model simulation of the Martian polar warming, Geophys. Res. Lett., 24 (2), 123.

Carbon Dioxide Convection in the Martian Polar Night and its Implications for Polar Processes. A. Colaprete[1] and R. M. Haberle[2], [1]SETI (NASA Ames Research Center, Moffett Field, MS 245−3, Mountain View,CA 94035, tonyc@freeze.arc.nasa.gov, [2]NASA Ames Research Center (NASA Ames Research Center, Moffett Field, MS 245−3, Mountain View,CA 94035).

Introduction: Each Martian year nearly 30% of the atmosphere is exchanged with the polar ice caps. This exchange occurs through a combination of direct surface condensation and atmospheric precipitation of carbon dioxide. It has long been thought the amount of condensation within the polar night is maintained by a balance between diabatic processes such as radiative cooling and latent heating from condensing CO_2. This assumption manifests itself in Mars General Circulation Models (GCM) in such a way as to never allow the atmospheric temperature to dip below the saturation temperature of CO_2. However, observations from Mars Global Surveyor (MGS) Radio Science (RS) and the Thermal Emission Spectrometer (TES) have demonstrated this assumption to be, at best, approximate. Both RS and TES observations within the polar nights of both poles indicate substantial supersaturated regions with respect to CO_2. The observed temperature profiles suggest conditionally unstable regions containing planetary significant amounts of potential convective energy. Presented here are estimates of the total planetary inventory of convective available potential energy (CAPE) and the potential convective energy flux (PCEF). The values for CAPE and PCEF are derived from RS temperature profiles and compared to Mars GCM results using a new convective CO2 cloud model that allows for the formation of CAPE.

CO_2 Convection: A rising air parcel will cool along the dry adiabat until saturated (Level of Condensation Lifting) at which time condensation and the release of latent heat force the parcel to cool along the wet adiabat. If the release of latent heat maintains the air parcel temperature above the environment temperature then it can become buoyant and freely convect (Level of Free Convection). Free convection will continue as long as the parcel remains warmer than its surroundings (Level of Neutral Buoyancy). The amount of free convection that can occur depends on the difference in temperature between the ascending air parcel and its environment. One measure of the ability of a parcel to freely convect is the convective available potential energy (CAPE). The CAPE of a parcel can be expressed as

$$CAPE = \int_{z_1}^{z_2} b\,dz \qquad 1.$$

where z_1 and z_2 are the initial and ending altitudes of the rising parcel of air and b is the buoyancy

$$b = g\frac{(T_p - T_e)}{T_e} \qquad 2.$$

with T_p and T_e being the temperature of the parcel and environment respectively. Within the Martian polar night the atmosphere is frequently at or above the CO_2 saturation temperature. If an air parcel near the surface is forced to rise it will very quickly become saturated and cool along the wet adiabat. However, since the surrounding atmosphere is already at the wet adiabat the parcel's buoyancy is nearly zero ($T_p - T_e \approx 0$). Therefore there is very little CAPE (with respect to CO_2 convection) within the Martian polar night and CO_2 convection would be shallow.

Not all of the Mars polar night atmosphere is at or above the saturation temperature, however. RS measurements indicate regions of CO_2 supersaturation in the lower atmosphere below about 1−2 mbar. Examples of RS observations showing supersaturations are shown in Figure 1. In Figure 1 four RS measurements, two for the South polar region and two for the North polar region, are shown with their corresponding CAPE (J kg^{-1}). These supersaturated regions can form if the air in the region is clear of any previously existing CO_2 cloud particles and new cloud particle nucleation has not yet occurred, or if atmospheric cooling rates are so high that the release of latent heat from growing CO_2 cloud particles is insufficient to compensate for the decrease in temperature. Under these conditions a rising parcel may be buoyant and will rise if condensation occurs. The CAPE for the profiles shown in Figure 1 varies from about 35 −250 J kg^{-1}. For comparison moderate to strong terrestrial convective systems have CAPE in the range from 500−1000 J kg^{-1}. Larger terrestrial thunderstorms can have CAPE greater than 2000 J kg^{-1}. On Earth, for similar amounts of CAPE as that calculated from the RS soundings in Figure 1, low to moderate levels of convection resulting in unorganized microbursts would be expected.

RS Observations: In the 6921 RS profiles analyzed thus far, approximately 25% of them show some amount of CAPE (as defined by Eq. 1). Figure 2 shows the location of the RS profiles which

contained CAPE. The highest value of CAPE was in the North and had a value of 421 J kg^{-1}. If all 421 J kg^{-1} of CAPE in this profile was converted to convective motion (neglecting entrainment effects and possibly cloud particle drag) the resulting updraft would have a velocity of almost 30 m s^{-1}. The total integrated CAPE in the profiles shown in Figure 2 is approximately 28 kJ kg^{-1}. Due to the limited spatial and temporal nature of the observations, the temperature profiles studied only constitute a fraction of the total atmospheric volume and time that CAPE is present. An estimate of the total rate of CAPE formation was made by linearly interpolating, in time and space, observed CAPE tendencies between observation points. Assuming all CAPE is converted to heat a total potential convective energy flux (PCEF) was calculated and is shown in Figure 3. The periods of highest PCEF correspond to the mid to late winter periods at both poles. The PCEF magnitude is largest in the North being about twice that of the South. During the late winter period the PCEF constitutes approximately 10% the total latent heating budget, or approximately equal to the total meridional heat transport.

A new CO_2 cloud model recently implemented in the Ames GCM reproduces the observed supersaturated regions. The cloud model includes the microphysical processes of nucleation, condensation, and sedimentation. Proper treatment of ice nuclei (IN) nucleation, assumed here to be dust grains, is critical to reproducing the observed supersaturated regions. The supersaturation at which new CO_2 cloud particles will form was recently measured to be 35%, consistent with the maximum supersaturations observed in the RS temperature profiles. Integrated CAPE and PCEF from simulations utilizing this new CO_2 cloud model are consistent with those estimated from the observations.

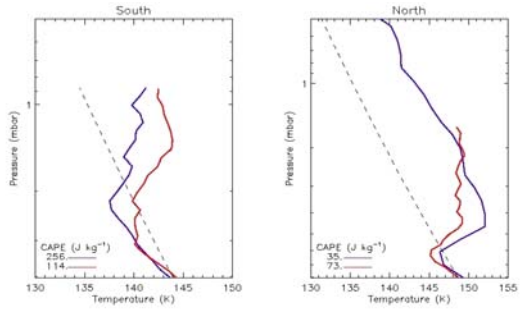

Figure 1. Examples of RS profiles (red and blue curves) showing supersaturated regions and the corresponding CAPE. The dashed curve is the frost temperature for CO2.

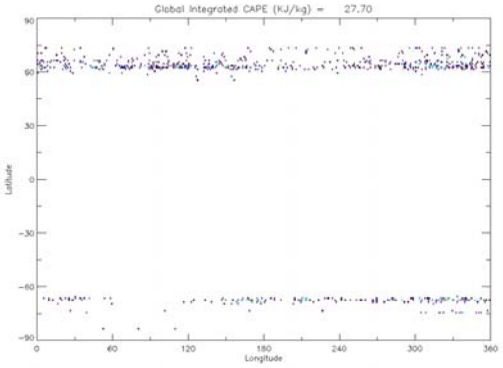

Figure 2: Location of RS profiles having CAPE associated with them.

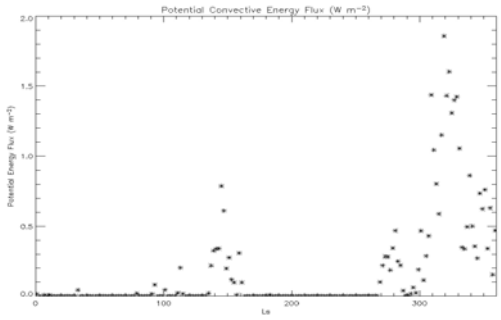

Figure 3. The estimated potential convective energy flux (PCEF) calculated from the total CAPE associated with all RS observations.

INTERANNUAL ATMOSPHERIC VARIABILITY SIMULATED BY A MARS GCM: IMPACTS ON THE POLAR REGIONS. Alison F.C. Bridger[1], R. M. Haberle[2] and J. L. Hollingsworth[3]: [1]Department of Meteorology, San Jose State University, San Jose CA 95192-0104, USA (bridger@met.sjsu.edu); [2,3]NASA Ames Research Center, MS 245-3, Moffett Field, CA, 94035-1000, USA (robert.m.haberle@nasa.gov, jeffh@humbabe.arc.nasa.gov).

Abstract: It is often assumed that in the absence of year-to-year dust variations, Mars' weather and climate are very repeatable, at least on decadal scales. Recent multi-annual simulations of a Mars GCM reveal however that significant interannual variations may occur with constant dust conditions [1]. In particular, interannual variability (IAV) appears to be associated with the spectrum of atmospheric disturbances that arise due to baroclinic instability. One quantity that shows significant IAV is the poleward heat flux associated with these waves. These variations – and their impacts on the polar heat balance – will be examined here.

Background: The dust loading of the martian atmosphere can vary significantly from location-to-location, from sol-to-sol, and from year-to-year. The surface dust reservoir varies too. However, were the surface and atmospheric dust distributions to remain fixed from one year to the next, it seems likely that the resulting atmospheric circulation at a give season would be repeatable from year-to-year. This follows from the absence of oceans on Mars.

We have recently conducted several multi-annual simulations with the NASA-Ames Mars General Circulation Model (MGCM; [2]). These extend for 10 years beyond a spin-up year (some 40 year simulations have also been performed). Some simulations have fixed dust all year (e.g., with a visible opacity of 0.5), while others have opacities varying through the year (e.g., following Viking observations). In these cases, the dust loading and distribution at a given *Ls* is the same during every year of the simulation. In a new series of simulations, we randomly specify the annual dust variation to fall between a low dust scenario (e.g., 0.3) and a high dust scenario (e.g., Viking)..

Results: In the first set of simulations (opacity fixed at 0.5 for all time), there is significant IAV in a number of parameters. For example, sol-averaged surface pressures at higher latitude sites (e.g., the Viking Lander 2 site) show variations of several tenths of a millibar from the 10-year average during the midwinter season [1]. This is an O(10%) variation from the long-time mean. Likewise, sol-averaged surface temperatures can be as much as 10-20 K above/below the 10-year average at these same sites. Such IAV is typical in the northern winter season at higher northern latitudes; it is far weaker in the corresponding southern winter season.

The region of high IAV is coincident with the location (in space and season) of baroclininc wave activity, suggesting a connection between the baroclinic wave activity and IAV. We have computed the poleward-directed heat flux $\left(\overline{v' T}\right)$ associated with these eddies (on Earth, this is a substantial fraction of the total poleward atmospheric heat flux). Figure 1 shows the resulting distributions of $\overline{v' T}$ computed over a 90 sol period centered on Ls 270 for each of the 10 years in the fixed opacity 0.5 simulation (the north pole is to the right on each plot, and the contour interval is 5 Km/s, with larger values shaded). Clearly, there are significant year-to-year variations in heat transport into the winter polar regions; the eddy heat flux in some years is virtually zero (e.g., years 01 and 08), whereas in other years values are O(30-40 Km/s). By comparison, poleward-directed heat fluxes associated with topographically-forced stationary waves have magnitudes O(10 Km/s) and show much less year-to-year variation [1].

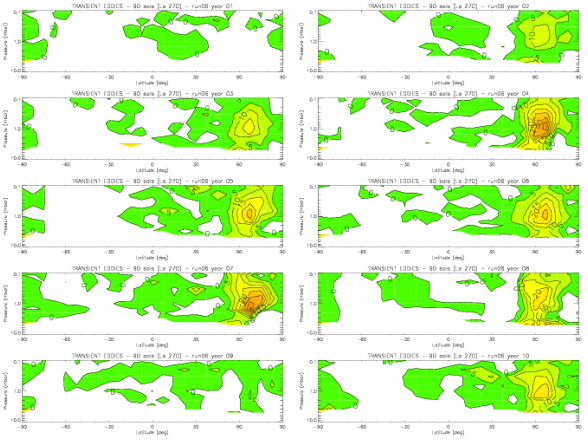

In the light of these variations in eddy heat fluxes into to winter polar region, we examine impacts on the polar heat budget. For example, the total accumulated ice mass in the northern polar region, computed as a function of *Ls*, deviates from the 10 year-average by up to ±O(3%) (Figure 2; each color represents a different year, and time is plotted a sol number, where sol 0 is *Ls* 0).

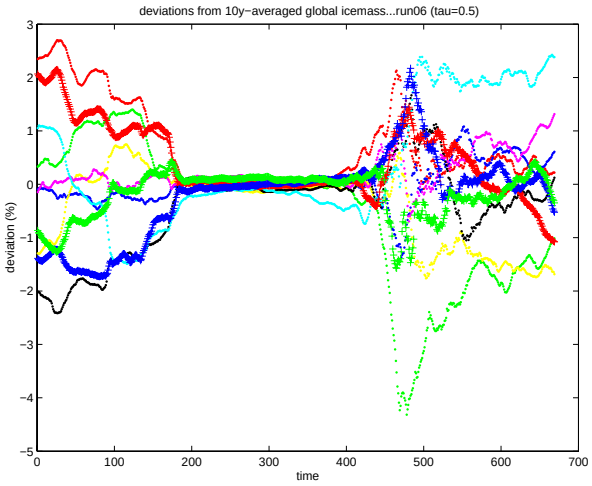

In this talk, we will expand upon the consequences of IAV for the polar region, with attention focussed on those quantities that might be detectable in long-term observations.

References: [1] Bridger,A.F.C., J. L. Hollingsworth, R.M.Haberle and S.R. Rafkin (2003), Granada workshop. [2] Haberle, R.M. *et al* (1999), JGR, 104, p. 8957.